3.1 Introduction

The apparatus for these current drive experiments was originally conceived as a tokamak type device with a toroidal vacuum vessel, a vertical field for equilibrium and a toroidal field for stability, but with RF coil structures for toroidal current drive replacing the inductive drive of the conventional tokamak.

Three such devices have been built during the evolution of the project. These devices were named Rythmac-1, Rythmac-2 and Rythmac-3 respectively. The dimensions of Rythmac-1, which was constructed to initiate the investigations, were constrained by budgeting requirements to utilise an existing toroidal magnetic field coil.

Following the initial successful current drive experiments with Rythmac-1, a larger (one and a half scale) device was designed. This machine was to become Rythmac-3. The motivation for building a larger scale machine was to produce a device which could sustain substantially higher driven currents with a current density similar to that in Rythmac-1. The larger vacuum vessel of Rythmac-3 permitted the magnetic field structure of the plasma to be studied with a relative increase in spatial resolution.

Rythmac-2 was an intermediate device with the same scale as Rythmac-1, which was built from the partially complete Rythmac-3 components. Rythmac-2 was constructed to test a different RF coil structure, which we have named the 'helical mesh antenna'.

Photographs of the Rythmac-1 and Rythmac-2 devices are shown in Figure 3.1 and Figure 3.2 respectively. The three devices, Rythmac-1,2,3, have many similarities in their technical features, which are described in the following sections.

3.2 The Discharge Vessels

The toroidal vacuum vessels for all three Rythmac devices were constructed in the Glassblowing Workshop at Flinders University from Pyrex glass tubing. The vacuum

Figure 3.1 A photograph of the Rythmac-1 apparatus.

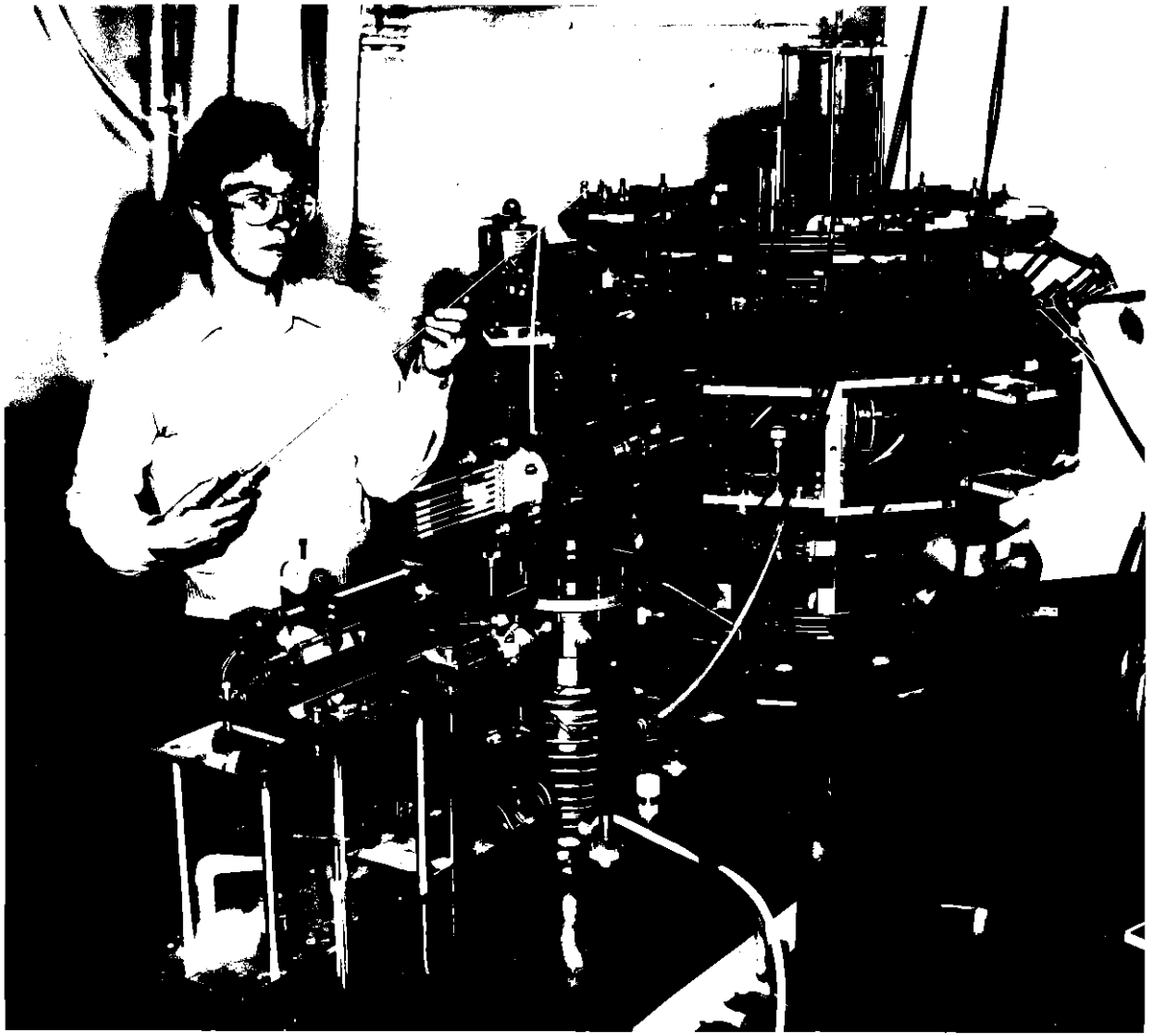

Figure 3.2 A photograph of the Rythmac-2 apparatus.

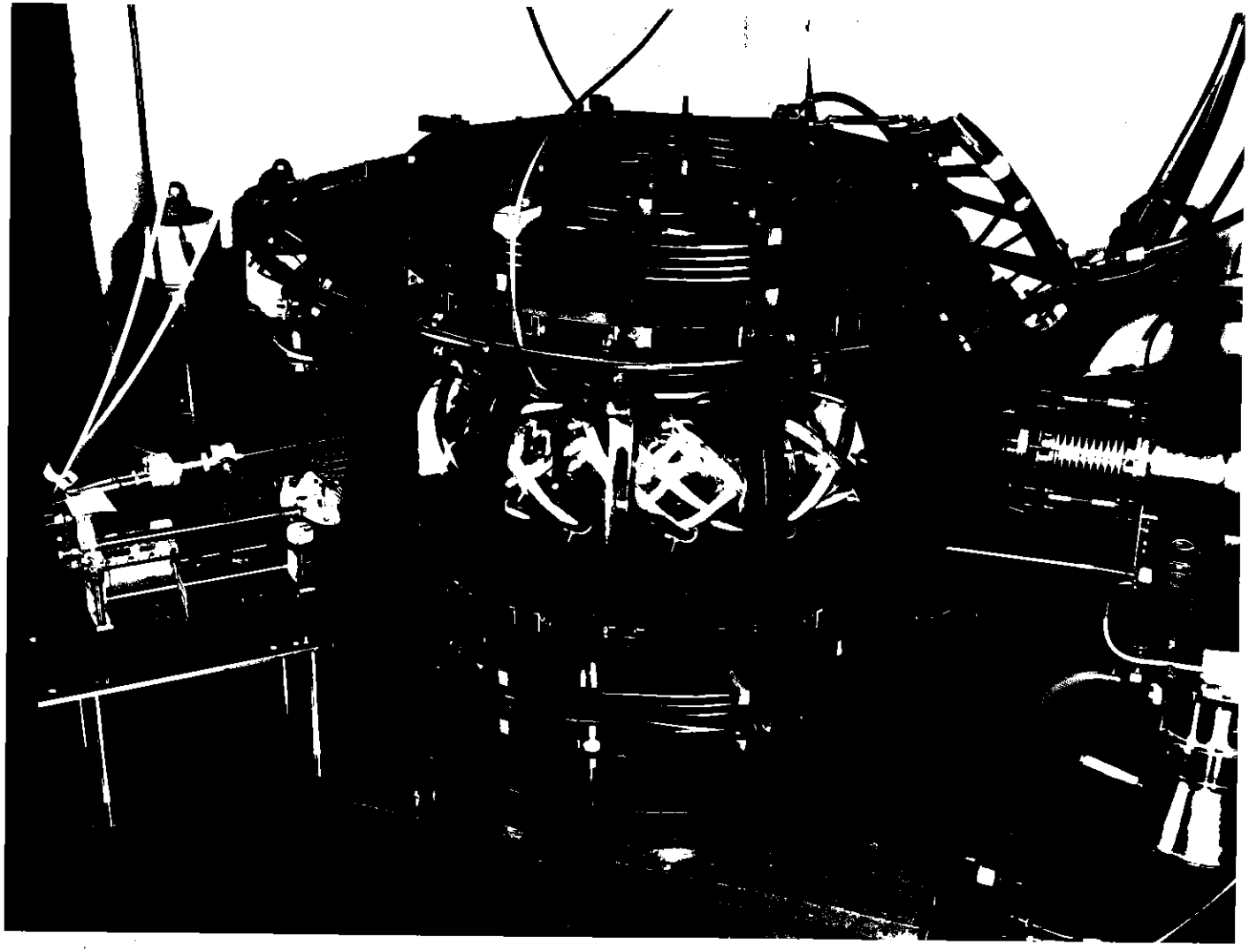

vessels for Rythmac-1 and Rythmac-2 each had a major radius of 25cm and a minor radius of 5cm. The larger Rythmac-3 device had a vacuum vessel with a major radius of 37.5cm and a minor radius of 7.5cm.

Wedge shaped pieces cut from straight Pyrex tubing as shown in Figures 3.3a,b were fused into toroidal sections and coupled together to form a fully toroidal vessel. All wedges were cut with a mean length of 10cm, which represented 1/16 of a complete torus in the case of Rythmac-1,2 and 1/24 of a torus in the case of Rythmac-3. To ensure easy assembly, each vessel was constructed from several toroidal sections which ranged in size from 67.5° (3/16 of a torus) to 135° (3/8 of a torus). Each section of glassware was equipped with commercially available (QVF) ground end flanges and two stainless steel coupling rings. In order to obtain a good vacuum seal, a Viton O-ring mounted in a stainless steel O-ring cage was placed between the end flanges of adjacent vessel sections which were then secured together with eight studs mounted through the stainless steel coupling rings as in Figure 3.3c.

The vessels for Rythmac-1 and Rythmac-2 were constructed from Pyrex glass tubing with an inner diameter (ID) of 105mm, an outer diameter (OD) of 115mm and a wall thickness of 5mm. The Rythmac-3 vessel was constructed from 151mm ID, 165mm OD Pyrex tubing with a wall thickness of 7mm. Each Rythmac vacuum vessel was equipped with a Pyrex glass pumping port of 75mm ID, 87mm OD fused to one of the toroidal vessel sections.

The Rythmac-1 vacuum vessel was constructed from four toroidal sections; two 1/4 sections, one 3/16 section and one 5/16 section, as shown in Figure 3.4a. One of the 1/4 sections was equipped with a pumping port constructed from a T-piece which housed an array of seven horizontal re-entrant probe guides (4mm ID, 6mm OD) with a vertical spacing of 1cm, as seen in Figure 3.1. The probe guides were used to insert a small magnetic probe into the minor section of the plasma. The other 1/4 section was placed in the opposite half of the torus and contained a 6mm OD stainless steel gas inlet line and four single probe guides (also 4mm ID, 6mm OD). Torr Seal low

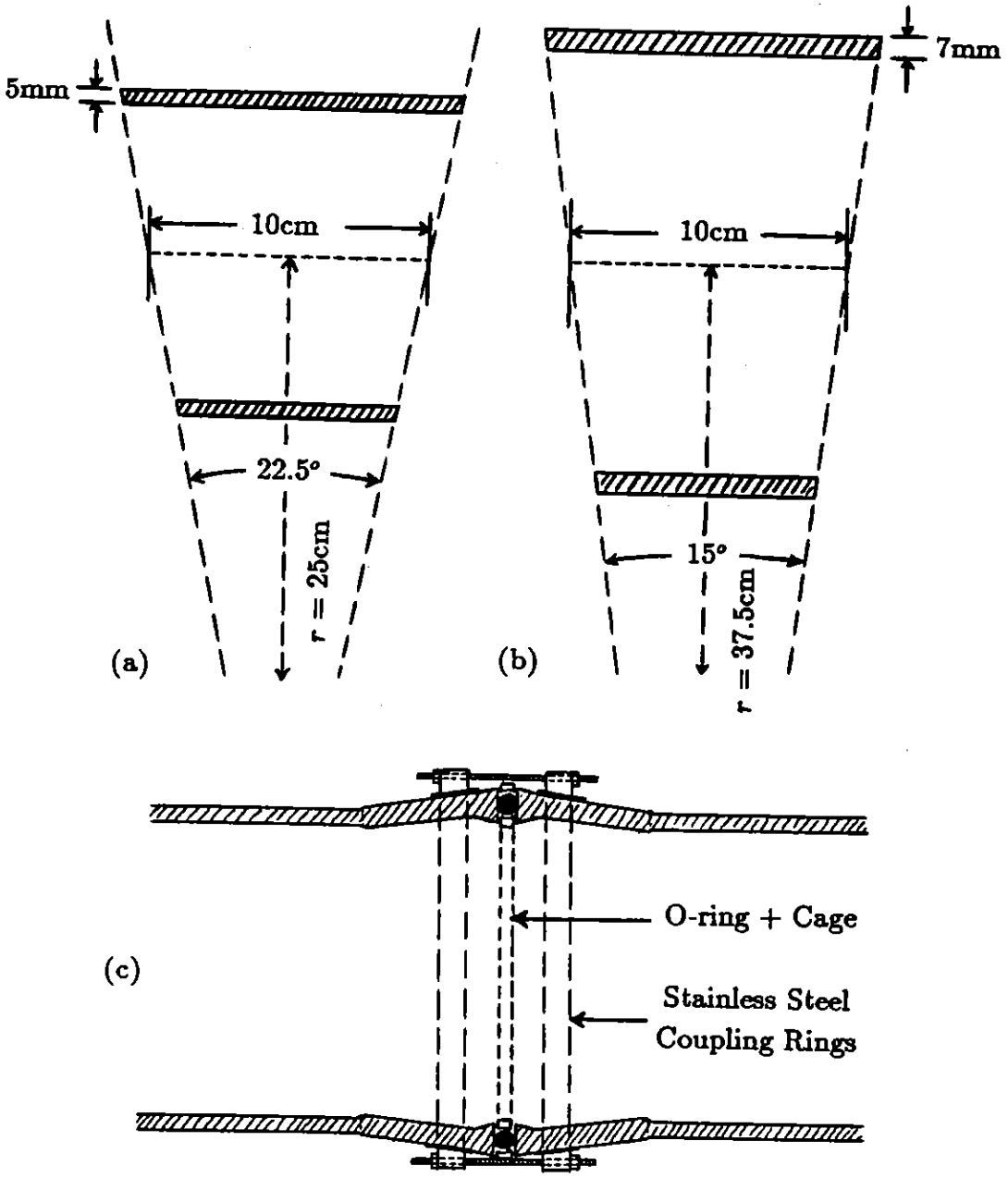

Figure 3.3 Vacuum vessel construction. Scale diagrams of the Pyrex glass wedges which were fused together to form the discharge vessels for (a) both Rythmac-1,2 and (b) Rythmac-3. Figure 3.3c is a schematic diagram showing the assembly designed to couple the toroidal vacuum vessel sections together.

vapour pressure resin was used to cement the probe guide housings onto the Pyrex glass vacuum vessel.

The vacuum vessel for Rythmac-2 shown schematically in Figure 3.4b was designed in three sections; one 1/4 section containing the pumping port and two 3/8 sections. One of the 3/8 sections was equipped with a Macor (machineable ceramic) block containing nine horizontal probe guides with a uniform vertical spacing of 1cm. The Macor block, which was also bonded to the glassware with Torr Seal resin, is visible in Figure 3.2 and is shown schematically in Figure 3.5.

The larger vacuum vessel for Rythmac-3 was manufactured in four quarter sections as shown in Figure 3.4c. One of the sections contained a 75mm ID pumping port whilst two of the remaining sections were each equipped with a Macor block containing thirteen re-entrant probe guides (4mm ID, 6mm OD) at a vertical spacing of 1cm, very similar in construction to the Macor block used on Rythmac-2. In order to minimize the amount of machining required and to reduce the risks of breakage or further weakening of the vacuum vessel, the feed point for the filling gas was relocated from the glassware onto the pumping line, directly above the pumps.

3.3 Vacuum System and Gas Handling

The pumping system for the Rythmac-1 device consisted of a 100mm Edwards diffstak (model 100) backed by a two-stage 5.0m^3/h Edwards rotary pump model E2M5. An ultimate base pressure of $\sim 10^{-6}$ mbar was measured with an Edwards ION7 ionisation gauge. A pneumatically operated 4″ (100mm) butterfly valve (Edwards model QSB4P) was mounted in the pumping line above the diffstak to isolate the discharge vessel from the pump whenever required. A schematic diagram of the Rythmac-1 vacuum system is shown in Figure 3.6.

The pumping system used for both the Rythmac-2,3 devices was recovered from the now dismantled FPS-2 linear machine and has been described previously by

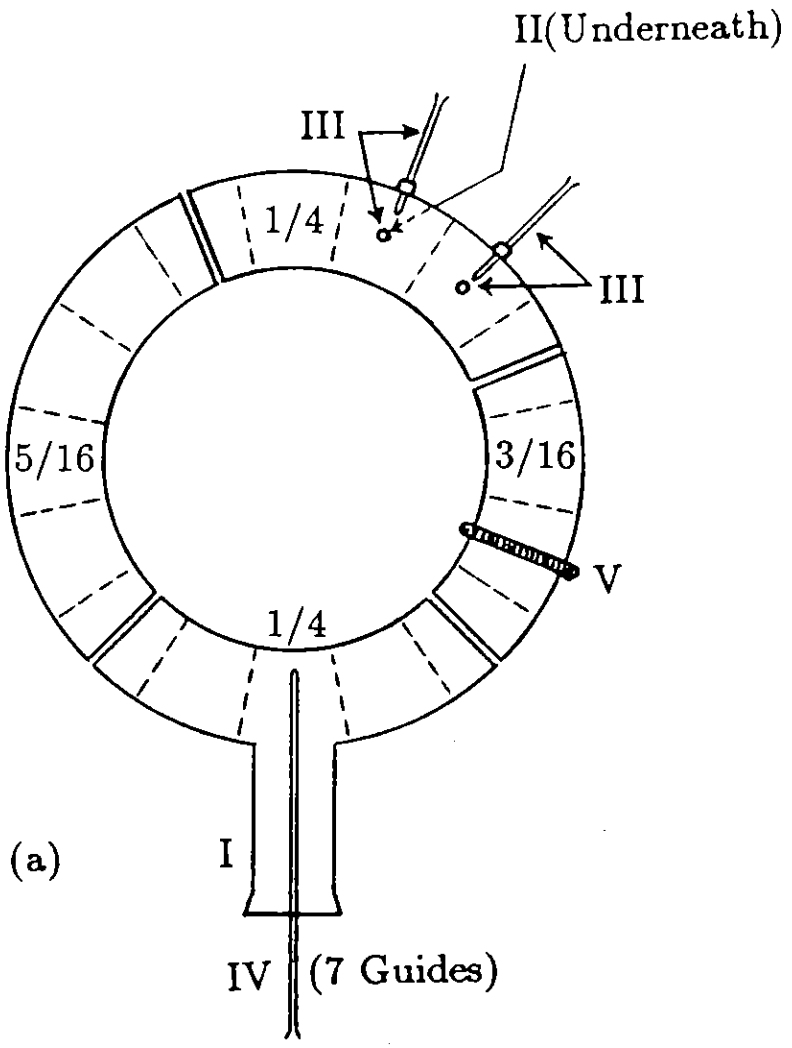

Figure 3.4 Schematic diagrams of the Rythmac vacuum vessel assemblies viewed from above, showing the relative locations of pumping port (I), gas inlet line (II), horizontal or vertical single probe guides (III), horizontal probe guide arrays (IV) and Rogowski belt (V), for each of the devices; (a) Rythmac-1, (b) Rythmac-2, (c) Rythmac-3.

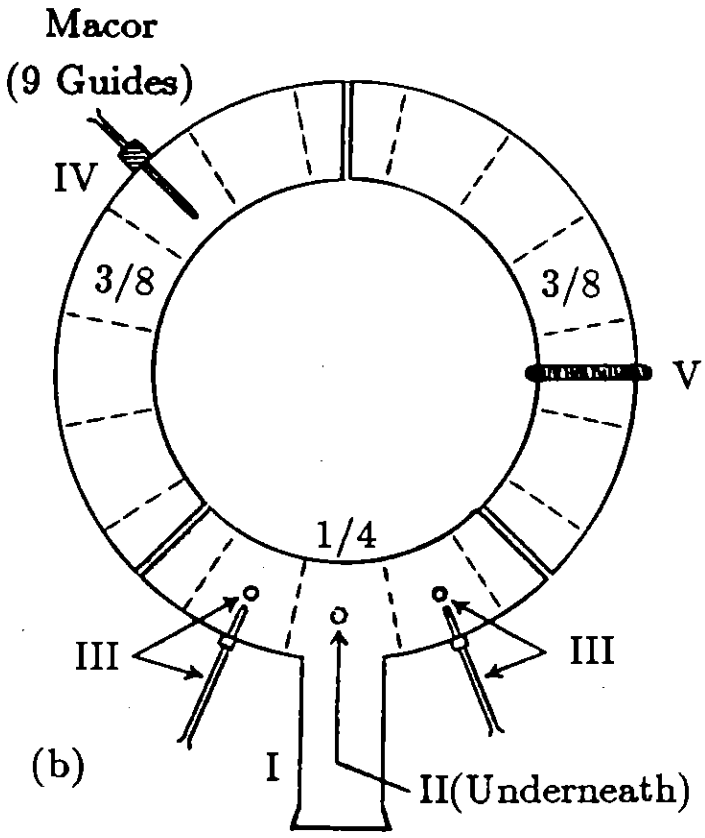

Figure 3.4b Caption reads as in Figure 3.4a.

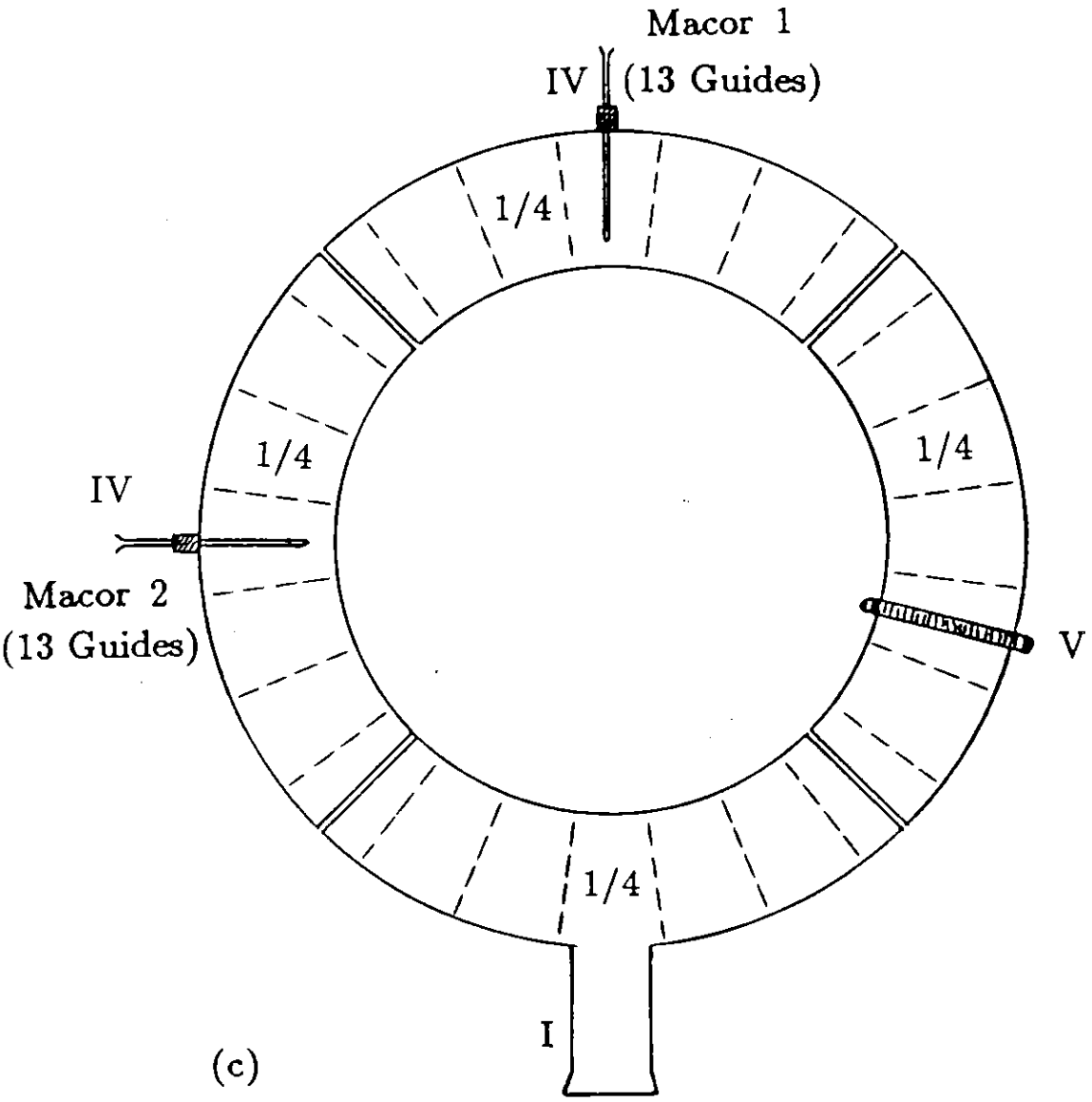

Figure 3.4c Caption again reads as in Figure 3.4a.

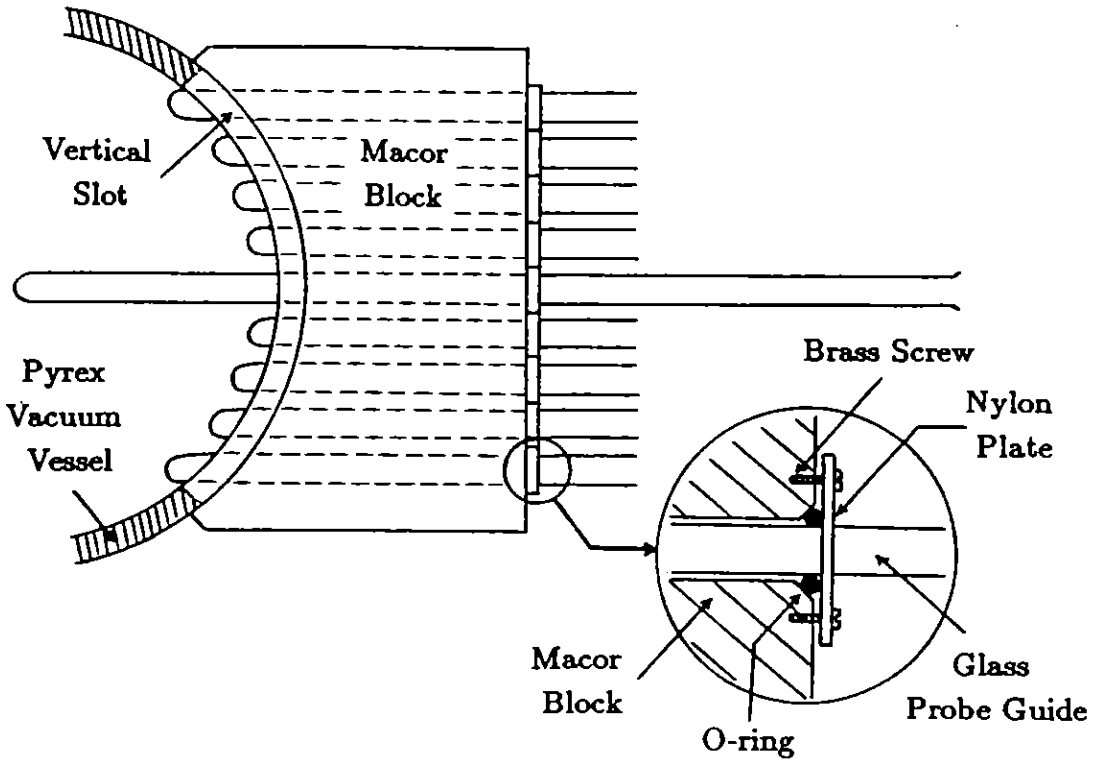

Figure 3.5 A schematic diagram of the Rythmac-2 Macor Block horizontal probe guide array. The probe guide spacing is 1cm. Two very similar Macor blocks were incorporated into the design of Rythmac-3. These Macor blocks contained 13 probe guides and O-ring cover plates machined from aluminium rather than nylon.

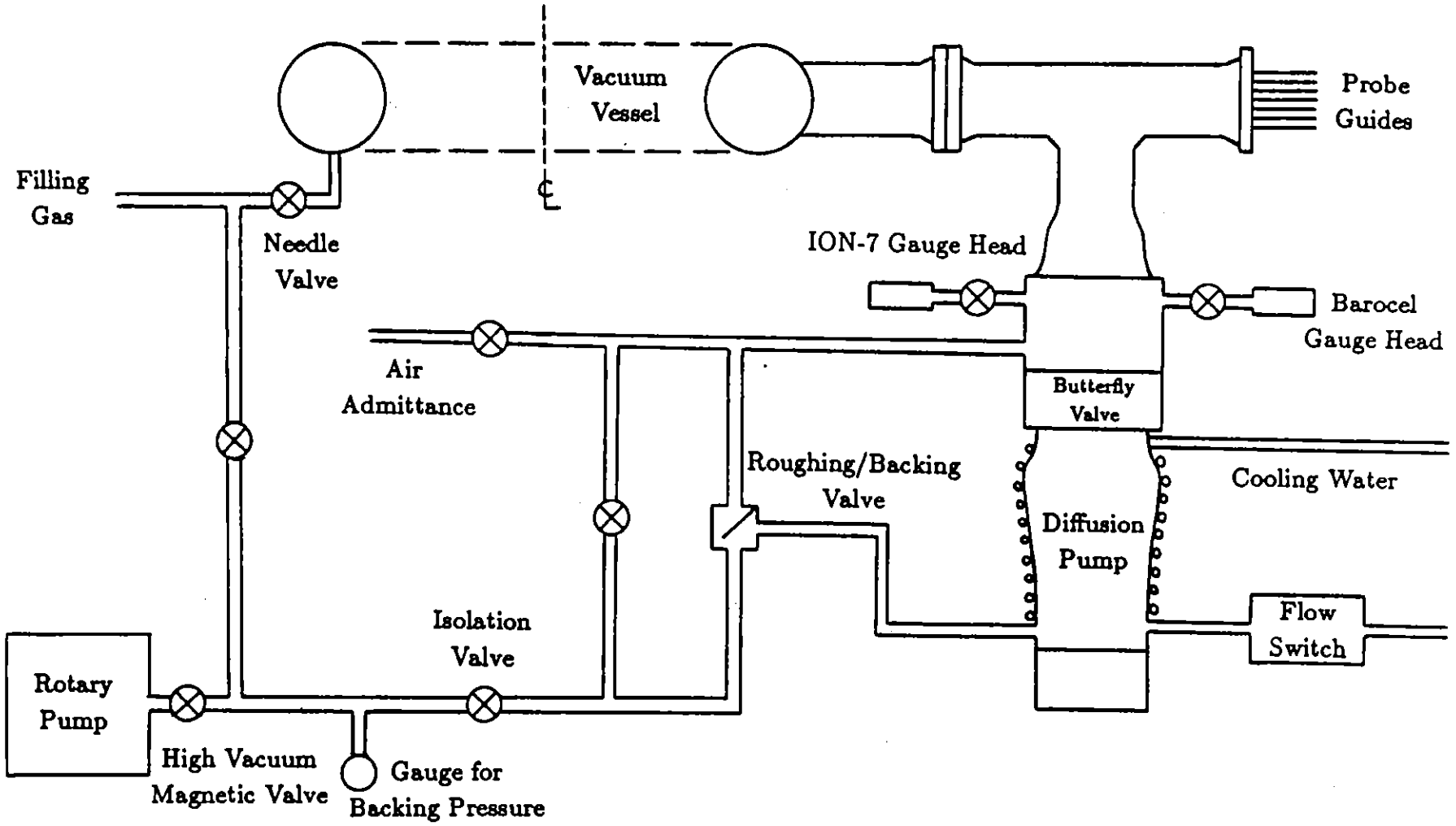

Figure 3.6 Schematic diagram of Rythmac-1 Vacuum System.

JESSUP(1977). The pumping station consisted basically of a 4″ (100mm) oil vapour pump (Edwards Speedivac model E04) fitted with a liquid nitrogen trap and backed by a two-stage rotary pump (Edwards Speedivac model ES150). The liquid nitrogen trap was not filled in the present experiments. This pumping system was able to achieve a base pressure of $\sim 2\times10^{-6}$ mbar in both Rythmac-2,3 as measured with the Edwards ION7 gauge. A pneumatically operated 4″ (100mm) butterfly valve located between the vacuum vessel and the diffusion pump was used to isolate the pumps from the vessel whenever necessary. The inlet for the filling gas was situated directly above the butterfly valve.

During all experiments on each of the three devices, the diffusion pump was throttled by partially closing the butterfly valve and the filling gas (Argon) was allowed to enter the vacuum vessel continuously through a Granville-Phillips needle valve. Throttling was found to be necessary in order to maintain the desired gas filling pressure (~1 mtorr in the vast majority of experiments) without choking the diffusion pump. The equilibrium gas pressure was controlled by the needle valve and monitored using a Datametrics Barocel electronic manometer (model 1173).

3.4 The Applied Toroidal Field

A steady externally-applied toroidal magnetic field B_ϕ is desirable for plasma stability and also aids in the initial breakdown of the filling gas. This magnetic field was generated by a fully toroidal solenoid which completely surrounded the vacuum vessel. The solenoid was constructed from a number of identical pancake coils each positioned at a mean spacing of 10cm around the circumference of the discharge vessel. The mean spacing between the field coils was chosen to be the same as the coil spacing in the earlier linear device, FPS-2, in order to obtain a field coil calibration on the major axis ($r=R_0, z=0$) similar to that stated by CHEETHAM(1976); 3 Gauss/Amp.

The variation of the steady normalised toroidal magnetic field in the major radial

and toroidal directions has been experimentally measured by DUTCH(1984) in the Rythmac-1 toroidal field coil structure. The normalised toroidal field profiles in the radial and toroidal directions are presented in Figure 3.7. The radial scans in Figure 3.7a were performed alongside one of the field coils (□) and bisecting two field coils (⊙). The broken curve shows the expected $1/r$ radial dependence of the field. Variation in the strength of the toroidal magnetic field with toroidal angle, as seen in Figure 3.7b, is caused by 'bulging' of the field between the pancake coils. The field variation in the toroidal direction is negligible on the major axis (r=25cm) but increases to approximately 6% at the outer wall of the vacuum vessel (r=30cm).

For the toroidal field profile measurements, the current through the toroidal field coils was supplied by a 'slow' capacitor bank, described in Section 3.5. The pulse length of the current was several milliseconds. A measure of the magnetic field strength was obtained by digitising and numerically integrating the output of a miniature wire-wound magnetic probe which is described in Chapter 4. The magnetic field measurements were normalised to the value of the field at the major axis (R_0=25cm).

In the case of Rythmac-1, the toroidal field solenoid was constructed from sixteen of the existing coils previously used to generate the axial magnetic field in the FPS-2 device. These pancake coils, which are described by JESSUP(1977), consisted of 25 turns of copper bar (9.7mm×6.3mm) spiralled on an inner diameter of 18.3cm and cast into modules with epoxy resin. The coils were 2.4cm thick with an outer diameter of 37.5cm.

New toroidal field coils with increased inner diameter were designed and constructed for use on Rythmac-3. For reasons of compatibility and ease of construction, these coils were designed to be the same physical size (37.5cm OD, 2.5cm thick) and have the same calibration (~3 Gauss/Amp) as the existing pancake coils. The coils, which were built in the Engineering Workshop on the same apparatus used to produce the original coils, consisted of 25 turns of copper bar (9.6mm×3.2mm) spiralled on an inner diameter of 26.4cm.

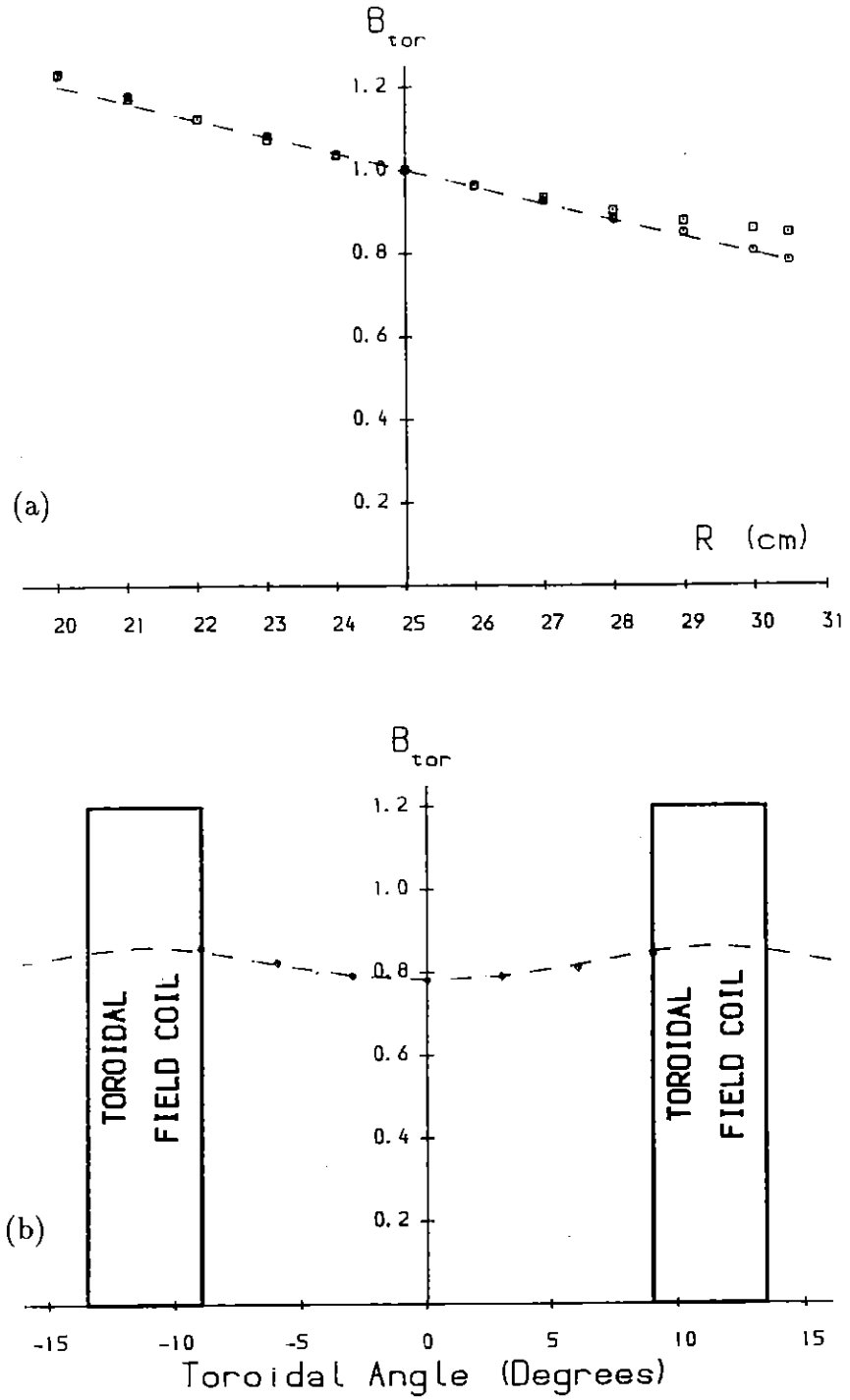

Figure 3.7 Experimentally measured (a) major radial and (b) toroidal profiles of the normalised steady toroidal magnetic field produced by the Rythmac-1 toroidal field coil structure. All scans were performed in the midplane of the device ($z = 0$). The radial profiles (a) were performed alongside one of the field coils ($\square$) and bisecting two field coils ($\odot$). The broken curve indicates the expected $1/r$ radial dependence of the field. The toroidal profile (b) was measured at the radial position $r = R_0 + 5.5 = 30.5$cm. The broken curve is a smooth fit to the data.

Sixteen of the new coils were incorporated into the design of Rythmac-2 (as seen in Figure 3.2), so that the added clearance between the field coils and vacuum vessel made it possible to install a helical mesh antenna described later in section 3.6.3. Twentyfour field coils were employed in the construction of the larger device, Rythmac-3, so that a mean coil spacing of 10cm could be retained.

A DC toroidal magnetic field was used in all the experiments described in this thesis. The current through the toroidal field pancake coils was supplied by either of the two available DC power supplies; Robyn 32/105V, maximum rating 190A DC or Rectifier Transportable (type 37A) 28V, 200A continuous. The toroidal field coil current was continuously monitored using a DC ammeter with an appropriate range; 50A f.s.d. (type unknown) or Siemens 250A f.s.d.

3.5 The Applied Vertical Field

In order to achieve radial and vertical equilibrium in a conventional tokamak plasma, a correctly shaped steady vertical magnetic field, B_v, must be applied. A steady vertical magnetic field may also be necessary to contain the RF driven toroidal current in the present experiments. There is however, the possibility that in an RF driven tokamak such as the Rythmac device, the component of the RF magnetic pressure in the minor radial direction (i.e. $\langle \tilde{j} \times \tilde{b} \rangle_r$) may be sufficiently large to maintain equilibrium in the absence of any externally applied vertical magnetic field.

In each of the Rythmac devices, the desired vertical magnetic field was produced by passing a current through a pair of vertical field coils (see Figure 3.8) located an equal distance above and below the midplane of the machine. Each coil consisted of several turns of high-current welding cable (Olex T46 0.6/1.0 kV). In the case of both Rythmac-1,2 a second smaller pair of vertical field coils were connected in series with the main field coils. By changing the number of turns in either pair of vertical field coils, or the coil separation, it was possible to adjust the shape of the vertical field as

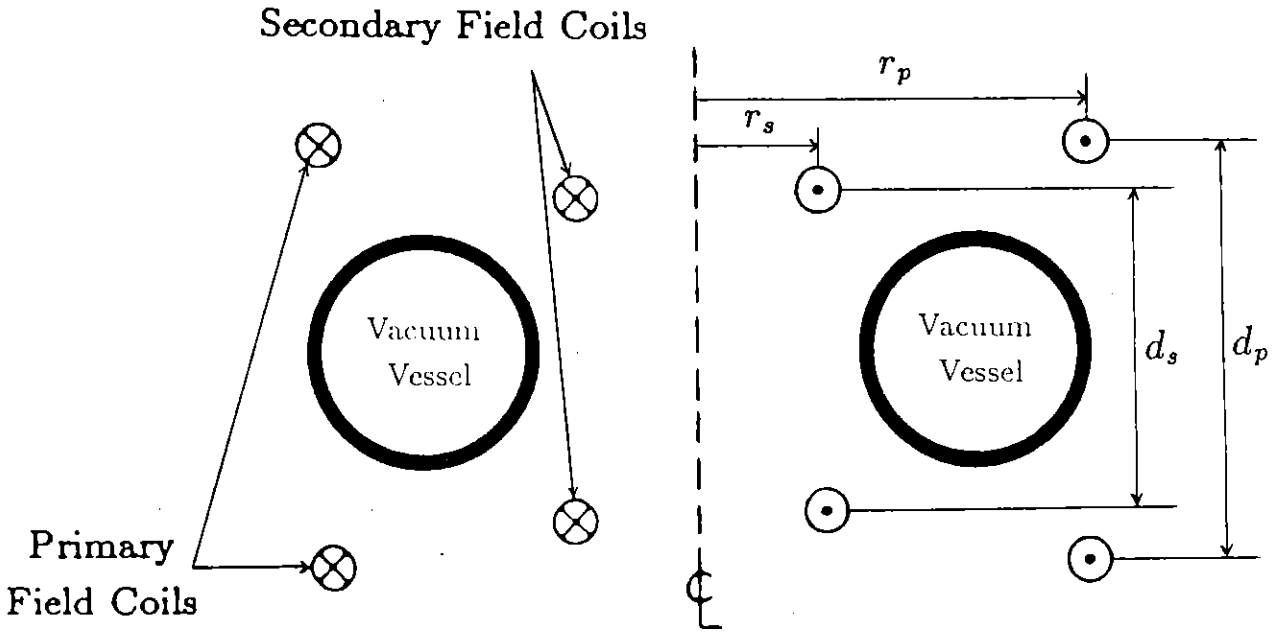

Figure 3.8 Schematic diagram of the Vertical Field Coil arrangement.

measured by the field index n where,

$$n(r) = \frac{r}{B_v(r)} \frac{\partial B_v}{\partial r}$$

For all the experiments carried out on both Rythmac-1,2 and early experiments on Rythmac-3, the vertical magnetic field was produced by discharging a 24kJ 'slow' capacitor bank through the vertical field coils. The designation 'slow' refers to the relatively long LC time constant (quarter period of several milliseconds depending on particular coil configuration) compared with the duration of the plasma ($\sim 50\mu$s). This capacitor bank was one of six identical units which comprised the slow bank originally used to generate the large pulsed axial magnetic field in the FPS-2 device. The bank consisted of ten 300μF capacitors assembled as two 1500μF units connected in series via a 5550 Ignitron switch. The bank could be charged to a maximum of 8kV however, the charging voltage used in the present experiments was typically only 300V, with the largest value used being 540V.

The current drive experiments (of approximate duration 50μs) were performed at the time of peak vertical magnetic field, after which the current in the vertical field coils was automatically crowbarred.

Later experiments on Rythmac-3 were performed with a DC vertical magnetic field generated by either of the two power supplies described in the previous section. This change in the nature of the applied vertical field was necessary because the slow bank ignitron switch did not operate reliably at very low slow bank charging voltages ($\sim$150V). Such low charging voltages would be required to produce desired values of vertical magnetic field which were considerably smaller than previously used. There was also the added disadvantage with the use of the slow bank that at such low charging voltages the absolute value of the charging voltage could not be selected with a reasonable degree of accuracy.

The vertical field coil specifications and slow bank calibration for each of the three Rythmac devices are given in table 3.1. The coil calibrations are the theoretical values calculated at the centre of the minor section ($r = R_0, z = 0$) using the known coil

TABLE 3.1

Vertical Field Coil Specifications.

device	primary field coil			secondary field coil			field index	coil calibration	slow bank calibration
	turns	r(cm)	d(cm)	turns	r(cm)	d(cm)	$n(R_0, 0)$	(G / A)	(V/A)
Rythmac-1	9	38.0	37.0	–	–	–	0.56	0.194	0.720
Rythmac-1	9	38.0	57.0	6	23.0	42.0	1.37	0.161	1.11
Rythmac-2	8	34.2	55.5	5	21.5	55.5	1.27	0.120	0.704
Rythmac-3	6	47.5	62.0	–	–	–	1.40	0.062	0.532

Note that field coil calibration is at $(R_0, 0)$.

dimensions and number of turns. The slow bank charging voltage/vertical field coil current calibration was determined by comparing the vertical magnetic field produced by the slow bank with the field produced at the same point when a known DC current was passed through the vertical field coils. A Hall effect magnetic probe (as described in chapter 4) was used to measure the field in each case.

3.6 The RF Field Coils

3.6.1 m=0 Coils

Initial investigations of RF current drive on Rythmac-1 were performed with $m = 0$ coils wound over part of the toroidal vacuum vessel. The present experiments differ from those of previous workers in the method of generating the RF travelling magnetic field. In the experiments of THONEMANN et al.(1952) and later work by FUKUDA et al.(1976) in their Synchromak device, the RF magnetic field was generated by a single RF source fed into a helical delay line surrounding the vacuum vessel. In the present work, the RF travelling magnetic field is produced by two RF sources of the same frequency (330kHz) which are dephased by one quarter of a period and fed into a pair of $m = 0$ coil structures as shown schematically in Figure 3.9a. The coils, which have a well defined periodicity length, ℓ, are shown in the large aspect ratio cylindrical approximation for clarity.

Slightly more than 1kA of toroidal current was driven using $m = 0$ coils with a structure wavelength of 20cm. Increasing the structure wavelength to 40cm resulted in less toroidal current being driven. This is attributed to a reduction in the strength of the radial component of the RF field. The direction of toroidal current drive could be reversed by changing the relative phasing of the RF coil currents.

We discovered several major technical difficulties associated with the use of $m = 0$ coils in the present devices, which led to the initial experiments with $m = 0$ coils being abandoned in favour of the $m = 1$ double helix coils.

In the $m = 0$ current drive scheme illustrated in Figure 3.9a, the two RF generators were found to be quite strongly coupled through their loads. The mutual coupling in the loads made it difficult to obtain two RF line generator currents of approximately equal amplitude, with a phase difference of 90° throughout the entire shot. The $m = 0$ coils were also found to be strongly coupled to the toroidal field pancake coils. Under certain experimental conditions (e.g. with $m = 0$ coils located directly underneath pancake coils and line charging voltages greater than $\sim$ 20kV), electrical breakdowns were observed in the interior of some pancake coils and across their terminals. These breakdowns were also observed when the number of turns in the $m = 0$ coils was increased from two to three in an attempt to increase the strength of the RF fields.

3.6.2 m=1 Double Helix Antenna

The $m = 1$ double helix antenna used to drive both toroidal and poloidal current in the Rythmac-1 and Rythmac-3 devices is shown schematically in Figure 3.9b. The antenna consists of two pairs of $m = 1$ helical coils located 90° apart in the θ direction. A separate RF source is used to feed each pair of $m = 1$ coils. The two RF sources are of equal frequency and are dephased by one quarter of a period.

The toroidal mode number of the coils, which is defined as the number of turns that each coil makes in the poloidal direction for a single turn in the toroidal direction, was $n = 4$ for Rythmac-1 and $n = 6$ for Rythmac-3. These particular values were adopted in order to take advantage of the symmetry imposed by the toroidal field coil structure. The choice of $n = 4$ for Rythmac-1 was made for the further reason that the magnetic field would progress at $\sim 45^o$ which, using a simplistic argument about field line progression, was predicted to be the optimum angle for toroidal current drive. By the time that Rythmac-3 was built, the theory presented in Chapter 2 was well advanced, and it was known that $n = 6$ was closer to optimum.

In experiments such as $m = 1$ double helix RF current drive, where poloidal current is expected to be driven strongly, the direction of the applied toroidal magnetic

field is important and can be chosen to produce either a diamagnetic or a paramagnetic configuration. Because confinement in the minor section is expected to be better for the diamagnetic case, this configuration was studied almost exclusively in the present experiments.

3.6.3 $m = +and-1$ Helical Mesh Antenna

The helical mesh antenna, which was installed on the Rythmac-2 device, was designed and used to drive purely toroidal quasi-steady current by means of the non-linear Hall effect. The helical mesh antenna was constructed from a superposed set of $m = +1$ (righthanded) and $m = -1$ (lefthanded) double helix coils. The toroidal winding number was $n = 4$. Each of the two RF sources (dephased by a quarter of a period) fed one pair of $m = +1$ coils in series with one pair of $m = -1$ coils. The series connection of the $m = +1$ coils with the $m = -1$ coils could be made in such a way as to drive purely toroidal current or purely poloidal current. The $m = +and-1$ helical mesh antenna is shown schematically in Figure 3.9c.

3.7 The RF Sources

The high power (~5 MW), short duration radio-frequency current sources used in all the experiments outlined in this thesis were modified Weibel line generators. The construction and performance of the line generators is described in some detail by STEPHAN(1983).

Each of the two generators produced an RF pulse of $\sim 50\mu s$ duration containing 16 periods of approximately constant amplitude current at a frequency of 330kHz. The line generators were typically charged to 28kV for $m = 1$ double helix current drive experiments on Rythmac-1, whilst the line charging voltages for experiments on Rythmac-2 and Rythmac-3 were 28.5kV and 27kV respectively. In each case the charging voltage chosen was the largest voltage for which no electrical breakdown

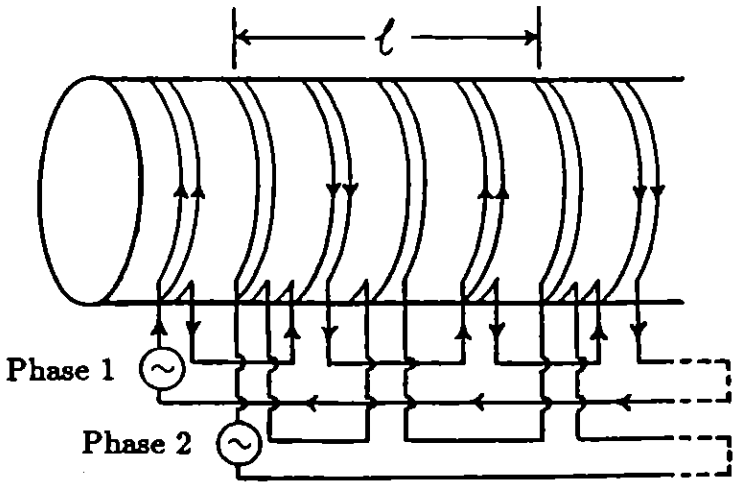

(a) The $m = 0$ coil structure used to drive purely toroidal current in the Rythmac-1 device.

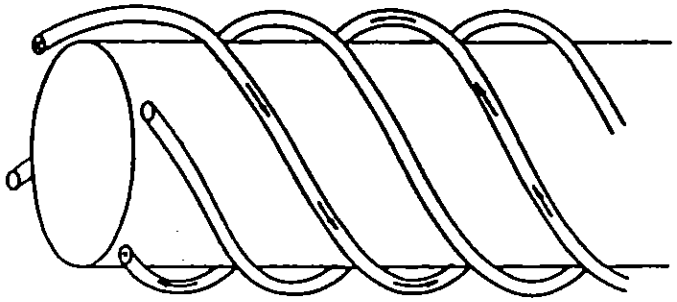

(b) The $m = 1$ Double Helix Antenna used to drive both toroidal and poloidal current.

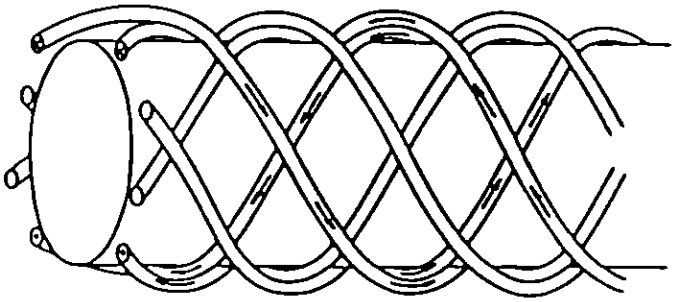

(c) The $m = +and-1$ Helical Mesh Antenna used to drive predominantly toroidal current in Rythmac-2.

Figure 3.9 Schematic diagrams of the various radio-frequency coil structures used to drive quasi-steady current by means of the non-linear Hall effect. The arrows indicate the direction of the r.f. currents at the instant when the current in phase 1 is maximum and the current in phase 2 is zero.

was observed in the line generator loads or the generators themselves. The charging voltage for initial $m = 0$ experiments on Rythmac-1 was limited to 20kV, due to breakdown in the toroidal field coils. The generators were charged using two HML 411-2250 automatic units. One charging unit was used to charge the positive plate of each generator, whilst the second charging unit was used to charge both negative plates.

A pair of matched externally integrated Rogowski belts originally constructed by STEPHAN(1983), were used to record the line generator current waveforms. The output of each Rogowski coil was integrated using a passive integrator with a 50Ω input resistor and an RC time constant of 33μs.

The integrated Rogowski signals were calibrated against a Model 1025 Pearson current transformer (0.025 V/A) at the line generator frequency of 330kHz. The calibration was performed by using both Rogowski coils and the Pearson to simultaneously measure the RF output current from one of the Line Generators. The sensitivity of each integrated Rogowski coil was found to be 300 ± 15mV/kA.

3.7.1 Load Tuning

STEPHAN(1983) has shown that the RF currents supplied by the line generators are largest for the longest length of time when the load circuits are tuned. Hence, tuning of the line generator loads was performed in the present experiments. However, it should be mentioned at this point that no attempt was made to match the load and generator impedances in any of the experiments described in this thesis.

The RF generators were used to supply suitably phased currents to the coil structures described in the previous section. Each coil structure possesses an inductance which would be completely tuned out by an appropriate series capacitance. In practice, a load capacitance consisting of one or more series 30nF capacitors (Thomson LCC C2498) was used. Where necessary, each generator load was individually fine tuned by adding extra load inductance using combinations of small fixed 2.2μH or

6.8μH inductors which are described by STEPHAN(1983).

The load tuning capacitor(s), C′, and fixed inductors, L′, were distributed throughout each load as shown in Figure 3.10, in order to minimize the voltages present in the load circuits. This was desirable to prevent electrical breakdowns to earth, or between the windings of the coil structure.

Tuning of the line generator loads was accomplished by monitoring the RF generator currents with the matched Rogowski belts whilst successively adjusting the tuning of one or both loads, until the 'best' RF current waveforms were obtained. The 'best' current waveforms were judged to be those where the RF currents maintained a large, approximately equal amplitude and a phase difference of $\sim 90^0$ for the longest length of time.

When the generator loads were correctly tuned (at the appropriate line charging voltage), the amplitudes of the RF coil currents were found to be approximately equal in each of the three devices. Figure 3.11 shows oscillograms of the two line generator current waveforms for a typical $m = 1$ double helix current drive plasma shot in Rythmac-1.

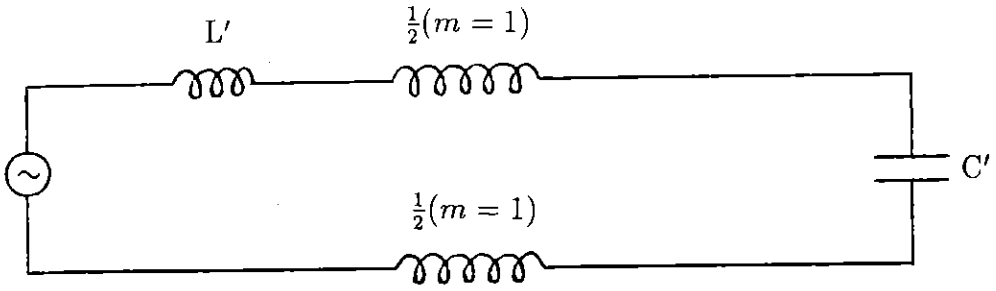

(a) Rythmac-1 : $m=1$ double helix antenna.

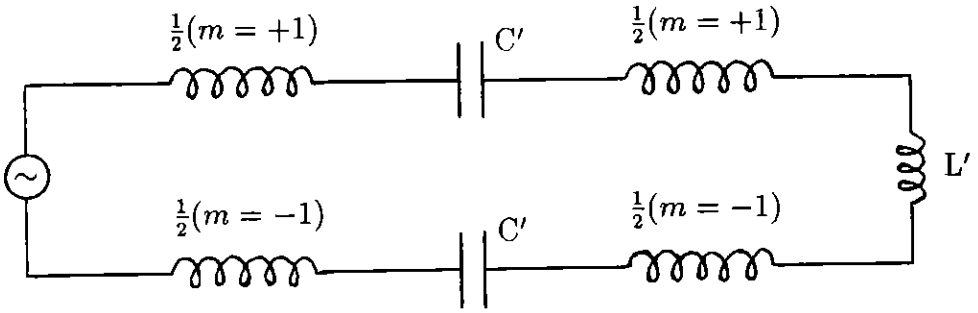

(b) Rythmac-2 : $m=+and-1$ helical mesh antenna.

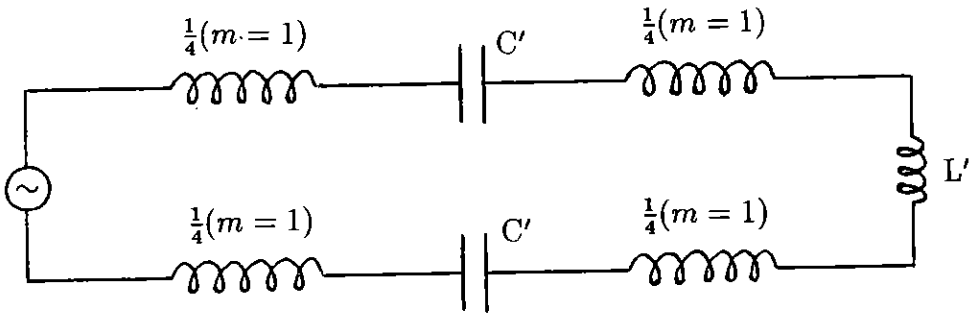

(c) Rythmac-3 : $m=1$ double helix antenna.

Figure 3.10 Schematic diagrams showing the location of the series tuning capacitor(s), C′, and fixed inductor combinations, L′, used to tune the helical RF coil structures which formed the line generator loads in each of the Rythmac devices. Note that only one of the two RF phases is shown in each of (a), (b) and (c).

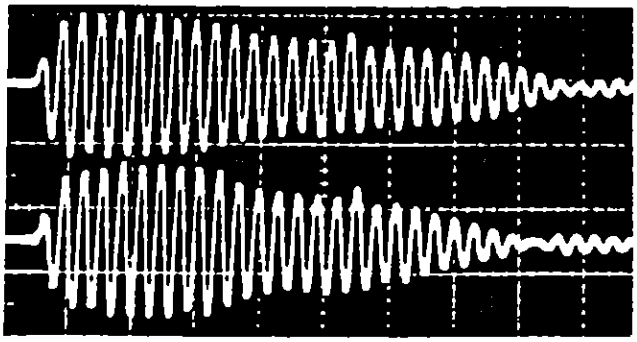

(a)

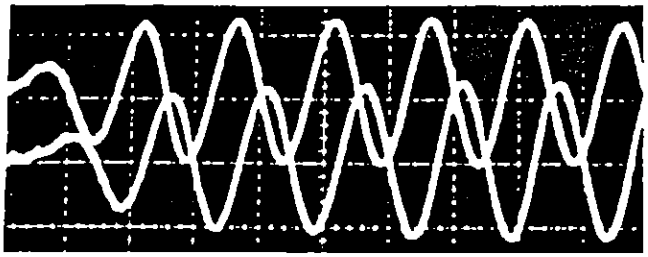

(b)

Figure 3.11 Oscillograms of typical Line Generator current waveforms in the Rythmac-1 device equipped with the $m = 1$ double helix antenna. The line charging voltage was 28kV. The vertical scale is 1.67kA/div. The timescale is (a) $10\mu s$/div and (b) $2\mu s$/div. Note the quarter period phase difference between the two currents.